Toward An MRI-Based Method to Measure Non-Uniform Cartilage Deformation: An MRI-Cyclic Loading Apparatus System and Steady-State Cyclic Displacement of Articular Cartilage Under Compressive Loading

C. P. Neu
Biomedical Engineering Graduate Group,
University of California at Davis,
Davis, CA

M. L. Hull[1]
Biomedical Engineering Graduate Group,
University of California at Davis,
Davis, CA;
Department of Mechanical and Aeronautical Engineering,
University of California at Davis,
Davis, CA

Recent magnetic resonance imaging (MRI) techniques have shown potential for measuring non-uniform deformations throughout the volume (i.e. three-dimensional (3D) deformations) in small orthopedic tissues such as articular cartilage. However, to analyze cartilage deformation using MRI techniques, a system is required which can construct images from multiple acquisitions of MRI signals from the cartilage in both the undeformed and deformed states. The objectives of the work reported in this article were to 1) design an apparatus that could apply highly repeatable cyclic compressive loads of 400 N and operate in the bore of an MRI scanner, 2) demonstrate that the apparatus and MRI scanner can be successfully integrated to observe 3D deformations in a phantom material, 3) use the apparatus to determine the load cycle necessary to achieve a steady-state deformation response in normal bovine articular cartilage samples using a flat-surfaced and nonporous indentor in unconfined compression. Composed of electronic and pneumatic components, the apparatus regulated pressure to a double-acting pneumatic cylinder so that (1) load-controlled compression cycles were applied to cartilage samples immersed in a saline bath, (2) loading and recovery periods within a cycle varied in time duration, and (3) load magnitude varied so that the stress applied to cartilage samples was within typical physiological ranges. In addition the apparatus allowed gating for MR image acquisition, and operation within the bore of an MRI scanner without creating image artifacts. The apparatus demonstrated high repeatability in load application with a standard deviation of 1.8% of the mean 400 N load applied. When the apparatus was integrated with an MRI scanner programmed with appropriate pulse sequences, images of a phantom material in both the undeformed and deformed states were constructed by assembling data acquired through multiple signal acquisitions. Additionally, the number of cycles to reach a steady-state response in normal bovine articular cartilage was 49 for a total cycle duration of 5 seconds, but decreased to 33 and 27 for increasing total cycle durations of 10 and 15 seconds, respectively. Once the steady-state response was achieved, 95% of all displacements were within ± 7.42 μm of the mean displacement, indicating that the displacement response to the cyclic loads was highly repeatable. With this performance, the MRI-loading apparatus system meets the requirements to create images of articular cartilage from which 3D deformation can be determined.
[DOI: 10.1115/1.1560141]

Keywords: Cartilage, Cyclic Loading, Load-Controlled, MRI, Steady-State, Displacement

Introduction

The experimental study of non-uniform deformation throughout the volume (i.e. three-dimensional (3D) deformation) of articular cartilage in response to loading is important to provide a comprehensive understanding of the properties of the normal and diseased tissue. Investigations of 3D deformation may provide an increased understanding of the process of mechanical signal transduction, where the 3D deformation of the extracellular cartilage matrix influences the deformation experienced by individual chondrocytes [1,2]. Experimental investigations of 3D deformation may also be useful in the verification of various analytical constitutive models [3] and computational models [4]. Moreover investigations of 3D deformation may allow for the detection of possible disease sites in the tissue by identifying localized areas where the stiffness of the tissue has changed from normal [5].

Methodologies that make use of magnetic resonance imaging (MRI) have demonstrated the ability to measure 3D cartilage de-

[1]Correspondence Address: Maury L. Hull, Ph.D., Department of Mechanical and Aeronautical Engineering, University of California, One Shields Avenue, Davis, CA 95616, phone: (530) 752-6220, fax: (530) 752-4158, email: mlhull@ucdavis.edu

Contributed by the Bioengineering Division for publication in the JOURNAL OF BIOMECHANICAL ENGINEERING. Manuscript received December 2001; revised manuscript received November 2002. Associate Editor: G. A. Ateshian.

formation noninvasively [6,7]. In contrast to previous experimental methods designed to investigate depth-dependent properties of cartilage [8–10], noninvasive MRI methods allow for experimentation without the use of excised samples. MRI methodologies have been employed to measure surface deformations (i.e. depth and volume changes) in cartilage both in vitro and in vivo [6,7,11–18]. However, to our knowledge no MRI-based methodology has been developed to measure 3D cartilage deformation throughout the volume of the tissue.

Unique motion-sensitive MRI pulse sequences, such as DANTE (Delays Alternating with Nutations for Tailored Excitation) [19], can potentially be used to identify and track the movement of specific surface and interior points hence enabling nonuniform deformations to be determined throughout the entire cartilage volume. This pulse sequence provides the ability to ''tag'' or label regions of tissue by locally perturbing the intrinsic magnetization of the tissue with a combination of magnetic field gradients and radio-frequency pulses. The labeled tissue regions (often appearing as a grid pattern of thin *tag lines* in images) may be tracked in sequential images and used to calculate deformation. Such techniques have been used primarily in cardiac applications [20–22], but have potential for calculating deformation in small orthopedic tissues such as articular cartilage.

While MRI provides an exceptional opportunity to examine 3D deformation, the realization of an MRI-based method to measure the 3D deformation of cartilage presents a unique set of challenges. An apparatus is required to load the tissue within the MRI scanner and must be constructed from materials (e.g. nonferromagnetic) that do not introduce any image artifacts. Further, the apparatus must impose cyclic loading on the cartilage while within an MRI scanner because a long period of time is required to image the thin cartilage (less than 5 mm thick on the tibial plateau) at a high spatial resolution (e.g. 50 μm). For example, it is estimated that a simple MRI fast spin echo acquisition of 3D data will take at least 16 minutes (repetition time: 3000 ms; phase encode steps: 512; echo train length: 16; number of excitations: 1; slices: 10). However, the tag lines created using the motion-sensitive MRI pulse sequences, and thus the contrast necessary to observe deformations, decay on the order of T_1 of the cartilage (770 ms at 1.5 T, and greater than 1000 ms at 7.05 T [23]). Because this time is considerably shorter than that required for the simple 3D MRI acquisition, the cartilage must be cyclically loaded to allow for the acquisition of portions of the data needed for a complete 3D image during each loading cycle. Over many cycles, the portions of data can be assembled and processed into complete 3D images. Thus, one objective of this study was to design an apparatus that applies cyclic compressive loads and operates in the bore of an MRI scanner. A second objective was to demonstrate that the apparatus and MRI scanner can be successfully integrated to observe 3D deformations in a phantom material with MRI properties similar to that of articular cartilage.

A potential problem in applying this methodology to measure cartilage deformation is that the tissue exhibits viscoelastic behavior (e.g. stress relaxation and creep) [24], and so motion artifacts may obscure MR images assembled over many loading cycles. Consequently, the loading cycle must be carefully chosen so that the deformation between successive cycles is repeatable. Previous investigations of cyclic creep indicate that after a number of cycles, biological tissues reach a steady-state, or repeatable deformation, in response to an applied load provided that the recovery period is sufficiently long [25]. Accordingly, the number of loading cycles necessary to achieve the steady-state response for a specific recovery period must be determined so that this number of loading cycles can be applied prior to imaging. Image acquisition during cyclic loading will commence once a steady-state displacement response has been achieved. Thus, the third objective was to develop a method for determining the number of load cycles necessary to achieve a steady-state displacement response for a viscoelastic material and to demonstrate the method using samples of normal bovine articular cartilage.

Methods

Cyclic Loading Apparatus Design. An apparatus was designed as an electro-pneumatic system to cyclically load cartilage samples inside an MRI scanner (Fig. 1). Pneumatically, the components consisted of a compressor (T-150HP, Thomas Industries Inc., Sheboygan, WI), pressure servovalve (QB1TFEE100-S896, Proportion Air, McCordsville, IN), solenoid valves (S5SS9D, IR Fluid Products, Bryan, OH), and a custom double-acting pneumatic cylinder. The operating pressure of the compressor was set at 0.76 MPa. The servovalve was capable of regulating the pressure between 0 and 0.69 MPa to the solenoid valves and cylinder. Additionally, the pressure servovalve was the key component in the system, as it regulated the pressure to a $\pm 0.2\%$ full-scale accuracy. Thus, the servovalve provided a consistent supply of pressure to the cylinder and allowed for consistent subsequent loading of cartilage samples. This component also allowed for the controlled application of various loading magnitudes by varying its pressure output.

Electrically, the apparatus was controlled by a computer running custom Visual C++ (v6.0, Microsoft Corporation, Seattle, WA) and data acquisition software (NI-DAQ; National Instruments Corporation, Austin, TX). A counter was established using the NI-DAQ software to allow for precise timing (10 μs resolution) of events in the system. The computer directly provided a command signal (between 0 and 10 V) to the servovalve to control the pressure to pneumatic components, and indirectly provided command signals (5 V) to the solenoid valves via electrical relays to control the direction of air flow to the cylinder, as well as the subsequent motion of the double-acting cylinder piston rod. The computer also provided a command signal (5 V) to the MRI scanner to trigger image acquisitions (discussed subsequently). Finally, a laser system (LB1101, Keyence Corporation, Woodcliff Lake, NJ) was mounted to the apparatus to monitor displacements of the piston rod. This laser system has been shown in our laboratory to measure displacement with a precision of ± 2.4 μm [26].

A loading mechanism was designed to load the cartilage samples within the restricted bore of the MRI scanner (Fig. 1(*B*)). The piston rod of the cylinder extended through a cantilever section of the loading mechanism to the tissue sample holder where loading occurred. Ultimately, the tissue will be loaded within a small horizontal MRI scanner bore, which is approximately 33 mm in diameter, in a Biospec 70/30 system with micro-imaging gradients (7.05 Bruker Medical GMBH, Ettlingen, Germany). The motion-sensitive MRI experiments to be described later were conducted on this system. With the loading mechanism interfaced to the MRI scanner, tissue samples (maximum geometry 21.6 $\times 18.0 \times 15.0$ mm^3) were placed at the scanner isocenter. If desired, then tissue samples could be submerged in a 0.15 molar sodium chloride solution to mimic the *in vivo* environment (Fig. 2(A)). To fix the cartilage to the apparatus, the tissue sample subchondral bone was attached rigidly using ethyl cyanoacrylate to an orthorhombic Delrin mount (geometry $21.6 \times 18.0 \times 3.8$ mm^3) (Fig. 2(*B*)). Additionally, a flat-surfaced and nonporous indentor was used to load the samples in unconfined compression.

The loading mechanism was constructed from materials that minimized the introduction of MR image artifacts. The cylinder was machined from Delrin, a material that has been used in previous studies of static loading inside an MRI scanner without detrimental effects [7]. Additionally, rubber cylinder diaphragms (KD-4L, Illinois Pneumatics, Roscoe, IL) were used with a molybdenum disulfide powder lubricant to provide a low-friction seal between the Delrin piston and the cylinder. However, other system components (e.g. compressor) were constructed from metallic

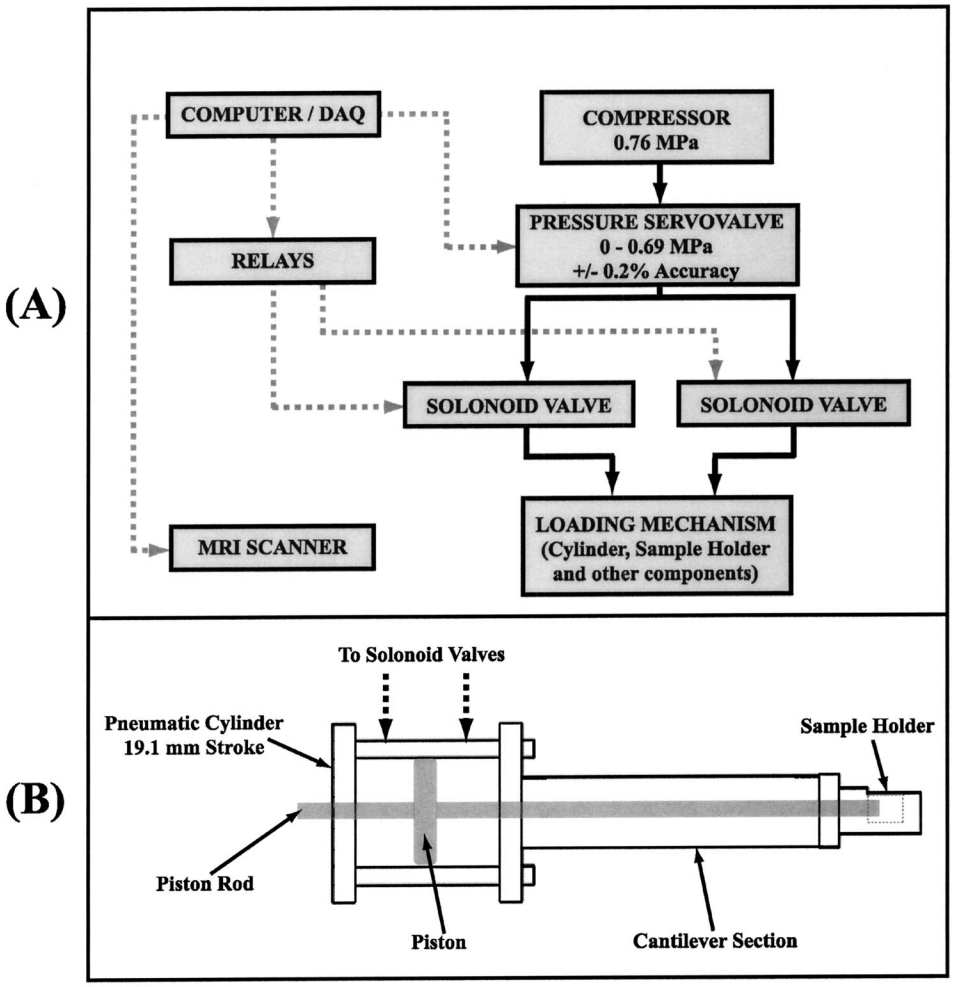

Fig. 1 Electro-pneumatic schematic (*A*) of the cyclic loading apparatus depicting the relationship between electronic (gray dashed arrows) and pneumatic (black solid arrows) components. Details of the loading mechanism are also shown (*B*), including the pneumatic cylinder, cantilever section, and sample holder. Rubber diaphragms (not shown) were used to provide a low-friction seal between the Delrin piston and the cylinder. A laser displacement measurement system (not shown) was also mounted to the apparatus.

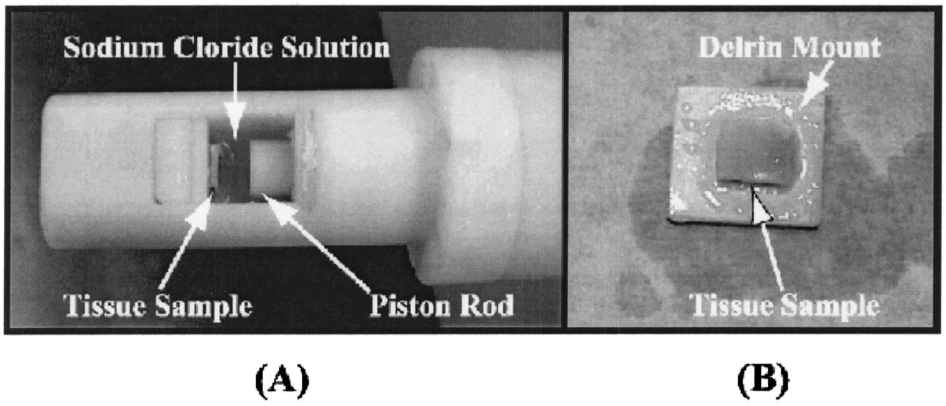

Fig. 2 Photographs of a cartilage sample within the sample holder (*A*) and affixed to a Delrin mount (*B*)

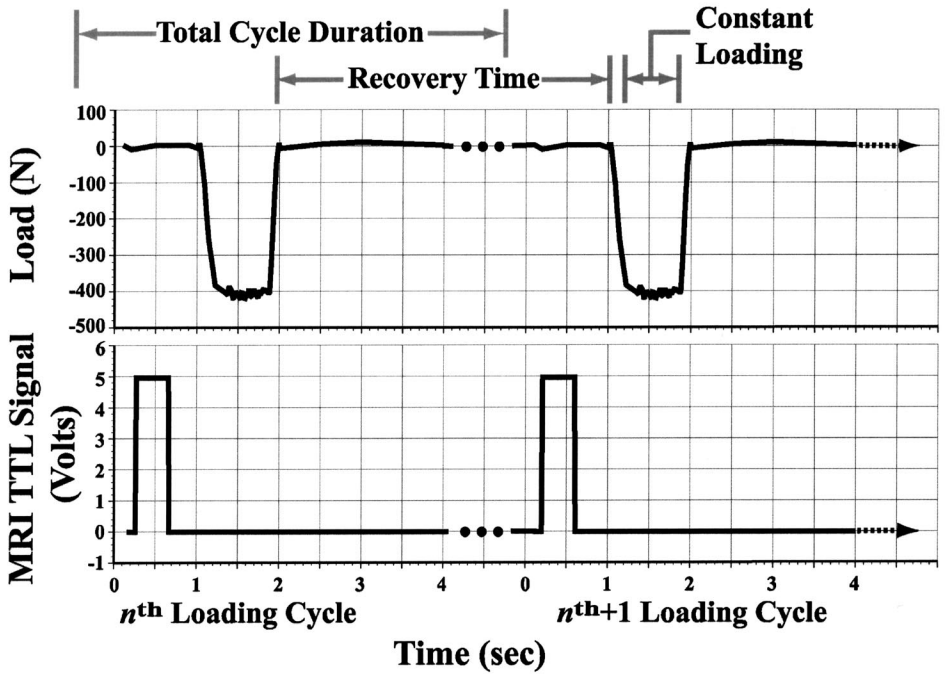

Fig. 3 Timing diagram of the compressive load application and MRI signaling for two arbitrary loading cycles. Load is applied once during each cycle with variable total cycle duration, recovery time, and interval of constant loading. A TTL signal is sent to the MRI scanner prior to the onset of compression to trigger the DANTE pulse sequence and image the cartilage sample both prior to and after deformation.

components. These components were connected to the pneumatic cylinder by plastic tubing greater than 2 m in length to ensure an adequate and safe distance from the scanner.

The cyclic loading mechanism provided uniaxial compressive loads to the cartilage. In a typical experiment (Fig. 3), the mechanism compressed the cartilage to a maximum load of 400 N which was achieved approximately 200 ms after load application commenced. This load magnitude was chosen because when applied over a typical sample area of 100 mm^2, a pressure of 4 MPa was created which can be developed easily on the tibial plateau of the human knee joint during walking [27,28]. The load magnitude, constant loading period, recovery time, and total cycle duration were all variable and computer-controlled.

A series of experiments were performed to determine the relationship between the load developed by the cyclic loading mechanism and the command signal given to the pressure servovalve by the computer. The load developed by the cyclic loading mechanism was measured in three independent experiments in which the command signal magnitude to the pressure servovalve was set at 2.5, 3.0 and 3.5 Volts. The mechanism compressed a load cell rated at a maximum load of 1112 N (LC307-250, Omega Engineering, Inc., Stamford, CT) ten times during each experiment with a 5-second total cycle duration. The load magnitude was averaged over all constant loading periods. The correlation coefficient was calculated from the load versus command signal data using a linear regression analysis.

Integration of the Apparatus and MRI Scanner. Integration of the cyclic loading apparatus and MRI scanner was accomplished via an electrical TTL trigger signal transmitted from the apparatus to the scanner (Fig. 3). This trigger signal synchronized the DANTE pulse sequence and image acquisitions directly to the compression cycles provided by the loading mechanism. Synchronization ensured acquisition of images with minimal motion artifacts. In a typical experiment (Fig. 3), one signal was sent to the MRI scanner prior to loading.

A phantom material (Sylgard 527 Silicone Dielectric Gel, Dow Corning, Midland, MI) was imaged in both the unloaded and loaded states to demonstrate the functionality of the MRI-cyclic load apparatus system for creating images assembled over repeated load cycles from which 3D deformations could be determined ultimately. This material has T_1 and T_2 properties similar to articular cartilage [29]. A phantom material rather than articular cartilage was used because the phantom material can also be used to verify the 3D strain calculations ultimately of interest. The apparatus was configured for a 20 N cyclic load magnitude (for the compliant gel) with a 5-second total cycle duration. The phantom material was imaged in an undeformed state just prior to the load application with a DANTE pulse sequence (to apply the tag lines) followed by a fast spin echo pulse sequence to create an image of the tag lines in the phantom material. The phantom was then deformed with the applied load, and then imaged again with a fast spin echo pulse sequence to capture the tag lines in a deformed state. The values of the DANTE and fast spin echo imaging parameters are given in the caption of Fig. 6.

Load Cycle for a Steady-State Response. Cartilage samples were tested to determine the load cycle to achieve a steady-state displacement response. Articular cartilage samples were harvested from the proximal metacarpals of four fresh-frozen normal adult bovine specimens. The harvested sample geometry was approximately 10.0×10.0 mm^2 cross-sectional contact area and 4.0 mm depth. The 4.0 mm depth consisted of approximately 2.0 mm of cartilage and 2.0 mm of underlying cortical bone. The cortical bone was not removed because it provided an effective rigid surface with which the sample was affixed to the apparatus. Inasmuch as the modulus of cortical bone exceeds that of the cartilage by more than 1000-fold [30], the deformation of the bone contributed negligibly to the deformation of the sample. Once harvested, the samples were attached to the Delrin mounts and refrigerated overnight prior to testing.

Cartilage samples underwent a specific unconfined and com-

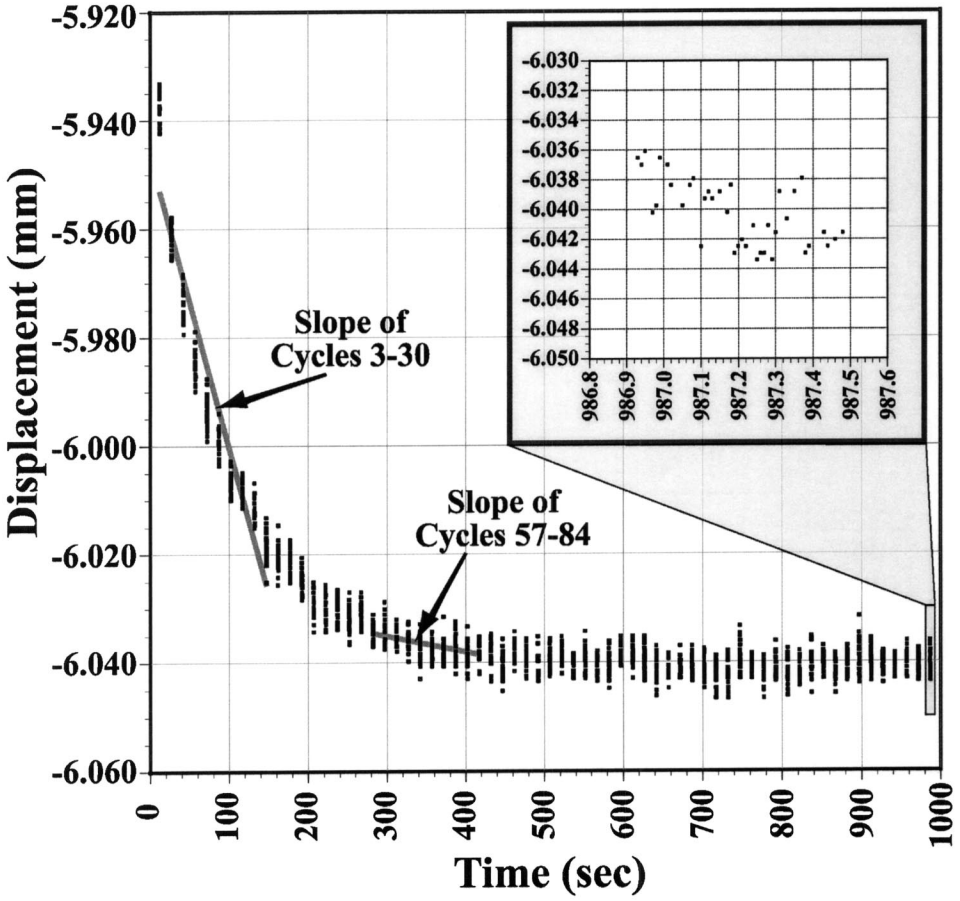

Fig. 4 Response of a typical cartilage sample to cyclic loading. Data for every third cycle was recorded and depicted. The slopes of two groups of cycles (3–30 and 57–84) are shown and were used to determine the cycle at which the cartilage sample reached a steady-state response. Based on a predetermined slope criterion described in the text, steady-state was determined to begin at cycle 57. An expanded view of cycle 198 shows a small amount of creep resulting from the period of constant loading.

pressive loading history on successive days to determine their steady-state viscoelastic response to the apparatus (Fig. 3). All cartilage samples were loaded with 200 cycles on respective days with a 1.5-second interval of constant 400 N loading during each loading cycle. The durations of the complete cycles were 5, 10, 15, and 5 seconds on days one, two, three and four respectively. Between successive days, the samples were immersed in a saline solution and allowed to recover overnight in a refrigerator. Because the results of testing on days one and four were not different (explained in the Results section), the overnight recovery was sufficient to fully recover the cartilage. The order of sample testing on any given day was randomized.

The number of cycles required to reach a steady-state viscoelastic response in the cartilage samples was determined using a predetermined slope criterion based on MR imaging parameters and a linear regression analysis to avoid motion artifacts in the images. The independent and dependent variables for the regression analysis were time and displacement, respectively. It was estimated previously that the total imaging time for a simple 3D MRI acquisition was 16 minutes. Assuming that 32 phase encode steps (e.g. 16 from two different slices each with an echo time of 6.8 ms) can be acquired during each loading cycle, the period of data analyzed during each loading cycle is only 217.6 ms, and the total number of loading cycles required for the 3D acquisition is 160 (512 [phase encode steps/slice]$\times$10 [slices]/32 [phase encode steps/loading cycle]). Further, we required that the total cyclic creep of the cartilage during the 160 cycles be no more than 25 μm, which corresponds to half of the desired high image spatial resolution of 50 μm. The criterion for reaching a steady-state response in the cartilage was that the slope of the regressed data be less than 25 [μm]/(total cycle duration [s/cycle] $\times$160 [cycles]) where the total cycle duration was either 5, 10 or 15 seconds, depending upon the test.

Inasmuch as data was recorded for every third cycle, groups of ten data cycles (i.e. 28 load cycles) were analyzed at a time using the aforementioned slope criterion and considered to represent the sample data. First the slope of cycles 3 through 30 was calculated and compared to the slope criterion. If the slope was greater than the criterion, then the slope of cycles 6 through 33 was analyzed. This process continued until the slope of a group of data cycles was less than the criterion. At this point, the first cycle of the group of ten was considered the cycle at which a steady-state response was achieved in the cartilage. The analysis described herein is illustrated in Fig. 4, where the slope of the cycles 3 through 30 as well as 57 through 84 are superimposed on typical data. The slope of the data for cycles 57 through 84 was less than the criterion, and thus the steady-state response for this particular data began at cycle 57. Further, the variability of the displacement data was investigated for all cycles for which the test was determined to be at steady-state. The range for which all of the displacement data was within 95% of the mean displacement was calculated using plus and minus two standard deviations. To

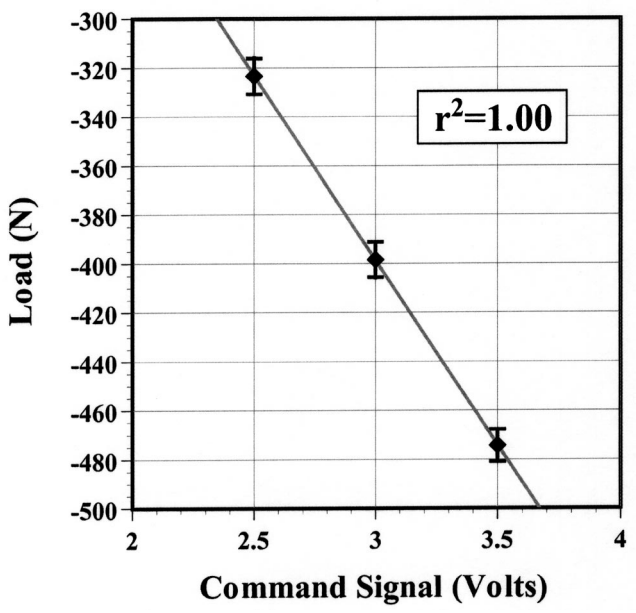

Fig. 5 Graph illustrating the highly correlated relationship between the load developed by the apparatus and the command signal sent to the pressure servovalve by the computer

verify that the cartilage samples were fully recovered on each day and to justify testing the cartilage on successive days, the means of the number of cycles necessary to reach steady state on days one and four (i.e. the two tests with identical total cycle durations) were compared using a paired *t*-test.

Results

A linear and highly correlated relationship was found between the load developed by the cyclic loading mechanism and the command signal given to the pressure servovalve by the computer (Fig. 5). The highest standard deviation was 2.3% of the mean 323 N load. Further, the standard deviation was approximately 1.8% of the mean 400 N load. These results indicate that cyclic cartilage loading may be accurately specified and controlled by the pressure servovalve.

Images of a phantom material were successfully captured with the use of the system created by integrating the cyclic loading apparatus and the MRI scanner with the pulse sequences (Fig. 6). The DANTE parameters produced a grid pattern of tag lines spaced approximately 1 mm apart. The fast spin echo parameters rested in voxel dimensions of $78\times78\times500$ microns^3 and were sufficient to demonstrate deformation of the phantom material. The timing of the apparatus and MRI scanner allowed for the acquisition, assembly, and visualization of images depicting the material in undeformed and deformed states. From these image data, detailed deformation information may be extracted.

Testing of the cartilage samples on successive days had no effect on the results presented in this study. The mean number of cycles needed to reach a steady-state response on day one (5 second total cycle duration) was 48.8 ± 10.8 cycles, and was nearly identical to the 49.5 ± 18.2 cycles needed to reach a steady-state response on day four (again, 5 second total cycle duration following 3 days of testing; $p=0.926$). Thus testing of samples on successive days was justified.

All of the cartilage samples tested ($n=4$) reached a steady-state response to the three different unconfined and compressive load cycles (Fig. 4). Qualitatively, the cartilage initially followed an exponential creep curve, but then reached a plateau region where no further noticeable creep occurred throughout the duration of the loading cycles. Also, an expanded view of the displacement versus time graph for the last cycle shows that less than 8 μm of displacement occurred during the period of constant loading.

The number of cycles needed to reach a steady-state response in the cartilage samples depended upon the total cycle duration (Fig. 7). For increasing total cycle duration, a decreasing number of cycles were needed in order to achieve a steady-state response. Once the steady-state response was achieved, 95% ($\pm$ two standard deviations) of all data was on average within ±7.42 μm of the mean, indicating that the displacement response to the cyclic loads was highly repeatable. Of note, this range of data included

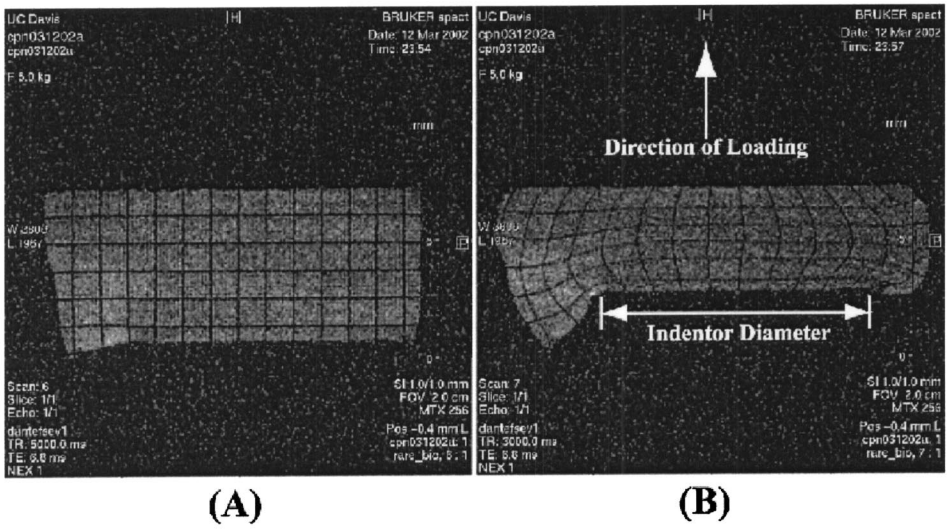

Fig. 6 Images of phantom material in undeformed (*A*) and deformed (*B*) states. DANTE tag lines are seen to deform with the tissue, thus permitting the calculation of deformation on the material surface and throughout the interior. DANTE imaging parameters were radiofrequency (RF) pulses=20; RF pulse duration=4 μs; inter-pulse duration=100 μs; magnetic field gradient strength=20.0 Gauss/cm. Fast spin echo imaging parameters were: TR=5000.0 ms; TE =6.8 ms; number of echoes per TR=8; field of view=2.00×2.00 cm^2; image matrix size=256×256 pixels^2; number of excitations=1; slice thickness=0.5 mm.

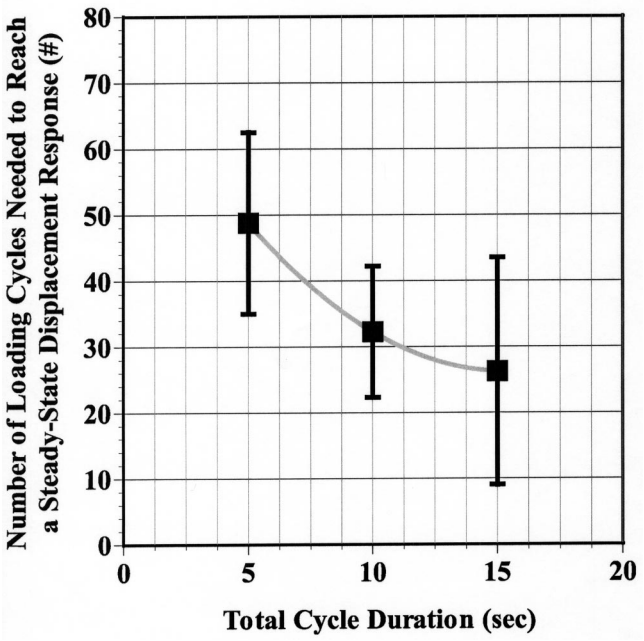

Fig. 7 Graph illustrating the relationship between the number of cycles needed to reach steady-state response in the cartilage samples and the total cycle duration

creep over all cycles for which the cartilage samples were at steady-state, as well as the creep during each constant loading period.

Discussion

This study was motivated by the need for detailed information regarding the non-uniform deformation of articular cartilage throughout the volume (i.e. 3D deformation) under compressive loading. Recent MRI techniques have shown potential for the measurement of 3D deformation in small orthopedic tissues such as articular cartilage. As steps in capitalizing on this potential, the objectives of this study were to 1) design and evaluate the performance of an apparatus to apply cyclic compressive loads and operate in the bore of an MRI scanner, 2) demonstrate that the apparatus and MRI scanner can be successfully integrated to observe 3D deformations, and 3) develop a method for determining the number of load cycles necessary to achieve a steady-state displacement response for a viscoelastic material and to demonstrate the method using bovine articular cartilage. The key results were that (1) the cyclic loading apparatus applied loads with high precision, 2) images of a phantom material in both undeformed and deformed states were captured using an MRI scanner and the apparatus thus demonstrating the potential to measure 3D deformation in cartilage, (3) cartilage samples reached steady-state response for all loading cycles specified herein, and (4) a decreasing number of cycles were needed in order to achieve a steady-state response as the total cycle duration (and thus the recovery time) was increased.

The apparatus provided repeatable loading within the magnetic environment of the MRI scanner. The small standard deviation (1.8%) of the mean 400 N load indicated that load-controlled compression was applied with good repeatability over many loading cycles using this apparatus. Further, although a 400 N load magnitude was used in this study, the load magnitude could be varied over a range of values. Based on the possible command signal values for the pressure servovalve (0–10 V range), and an extrapolation of the linear relationship found herein, it is reasonable to expect that load magnitudes may be specified between 0 and greater than 1000 N, although the relationship between the command signal and load magnitude may not be linear over this entire range. Additionally, the demonstration of the MR images of the phantom material (Fig. 6) indicates that the apparatus functioned and operated properly within the MRI scanner.

The cyclic loading apparatus used to cyclically load cartilage within an MRI scanner is unique in relation to previous cyclic loading apparatus designs. Previous designs have been implemented using a cam and follower assembly [31] and a load cell with microprocessor-based feedback [32]. Other designs have been employed to examine the biosynthesis response of cartilage during mechanical loading [33]. These previous designs were similar to the cyclic loading apparatus described herein in that they allowed for the application of a wide range of loads (as high as 500 N). Additionally, the previous designs allowed for rapid loading (as short as 20 ms in one apparatus). However, the previous designs typically employed metallic and electric components that rendered them inappropriate for our MRI application. A separate MRI-based study of cartilage deformation during static mechanical loading employed a pneumatic apparatus constructed in part from Delrin [7]. In contrast to the apparatus used in that study, our apparatus provides rapid and repeatable cyclic loading required for the MRI application discussed herein.

The integration of the cyclic loading apparatus and MRI scanner with the pulse sequences to capture images of the phantom material in undeformed and deformed states has several implications. First, the function of the apparatus was unaffected by the harsh MRI environment. Due to the design of the apparatus, this result was expected. Second, the phantom material used for demonstration in this study can now be replaced by other materials such as articular cartilage. When loaded appropriately and imaged using the MRI scanner with the pulse sequences, images can be assembled which illustrate deformations of tag lines throughout the volume of the cartilage.

Although it has been known for some time that biological tissues reach a steady-state response to cyclic loading [25], to the authors' knowledge the number of cycles needed to reach steady-state response for any loading cycle has not been specifically determined in cartilage. One study investigating the deformation response to cyclic loading of cartilage noted that specimens approached a steady-state response in as few as 200 cycles [34], although the specific number of cycles was not calculated. In contrast to that study, we found that the number of load cycles required to reach a steady-state response was less than 50 for the loading protocols specified herein, and that the number of cycles decreased as the total cycle duration (and hence the recovery time between cyclic loads) increased. Although the number of cycles to reach steady-state as a function of the recovery time was unknown, this result was expected based on the viscoelastic behavior of the cartilage in unconfined compression where rapid relaxation may be attributed to the ease of fluid flow from the tissue [35].

The steady state response of the cartilage to the cyclic loading applied by the apparatus is critical to the successful imaging of the cartilage within the MRI scanner. As mentioned previously, it is necessary that a sufficient number of preconditioning cycles be applied to the cartilage to avoid detrimental effects caused by the cartilage viscoelasticity which introduces motion artifacts in images acquired over long periods of time due to creep. The choice of such preconditioning cycles applied prior to imaging depends on the relationship between the number of cycles until steady state is achieved and the total cycle duration. Any of the three total cycle durations studied here are appropriate to achieve a steady state response prior to imaging. However, a 5-second total cycle duration is most appropriate if minimum total imaging time is desired. It is also important to apply more preconditioning cycles than the mean listed due to the variability observed between cartilage samples. A conservative estimate is the mean number of preconditioning cycles needed to reach a steady-state response plus two times the standard deviation. This amounts to 77 preconditioning cycles for a 5-second total cycle duration.

The usefulness of the steady-state data extends beyond the MRI application presented herein. The steady-state data may additionally aid in the experimental verification of theoretical constitutive models describing cartilage viscoelastic behavior. Specifically, this data may be compared to either analytic or numerical results of cartilage loading [4,35] in cyclic unconfined compression. The data presented is also valuable in experimental testing of cartilage to determine material properties (e.g. compressive modulus during cyclic testing) where knowledge of the number of preconditioning cycles prior to the steady-state response is necessary. However, the data is limited to normal bovine metacarpal cartilage explants, and further testing is required to determine the steady-state response in either normal human or diseased cartilage.

One unexpected behavior of the cartilage displacement response was that the nature of the response depended on the sample being tested. It was observed that the cartilage displacement response of the first sample tested on any given day did not match the exponential creep response of other samples shown in Fig. 4. The creep response of the first sample was typically exponential for approximately 20–40 cycles, then linear for approximately 15–30 cycles, and finally exponential for 15–30 cycles before reaching a steady-state response. The differences in the cartilage displacement response of the first sample tested can be attributed to an altered loading behavior of the apparatus. One possibility is that friction in the pneumatic cylinder changed during the initial loading cycles as the distribution of lubricant used with the rubber diaphragms in the cylinder also changed. As a consequence of this behavior, no data from the first sample tested on a particular day in this study was included in the analysis.

The result that the displacement response of the first sample tested on a given day was atypical has implications for the use of the apparatus when imaging cartilage in MRI experiments. One implication is that an additional number of cycles need to be applied prior to inserting the cartilage in the apparatus, thus allowing the apparatus to ''warm-up'' and hence avoid an unpredictable displacement response in the cartilage. Additionally, this result implies that the displacement response of the cartilage while in the MRI scanner should be monitored to ensure that the steady-state criterion has been met and that it remains satisfied. Accordingly the displacement response will be monitored using a fiber optic displacement sensor in future MRI experiments.

In summary, the contributions of this paper are as follows:

- The design of an MRI-compatible cyclic loading apparatus was described and the performance evaluation demonstrated both highly repeatable cyclic loading and functionality in an MRI scanner.
- The cyclic loading apparatus was integrated with an MRI scanner programmed with appropriate pulse sequences to produce a system which provided images of a phantom material in both the undeformed and deformed states assembled from repeated acquisitions during cyclic loading.
- A methodology for determining a load cycle to achieve steady-state cyclic displacement of viscoelastic materials was presented and the number of preconditioning loading cycles to achieve steady-state response in normal bovine articular cartilage was determined for three different load cycles.

Based on these contributions, the foundation is now laid to acquire images of articular cartilage in the undeformed and deformed states and determine the corresponding 3D deformations.

Acknowledgements

The authors thank Mike Akahori and David Hook for their machine shop assistance, and Nancy Emery for giving helpful comments on this manuscript. Support from National Science Foundation grant BES-0096436 is gratefully acknowledged.

References

[1] Buschmann, M. D., Gluzband, Y. A., Grodzinsky, A. J., and Hunziker, E. B., 1995, ''Mechanical Compression Modulates Matrix Biosynthesis in Chondrocyte/Agarose Culture,'' J. Cell. Sci., **108**, pp. 1497–1508.
[2] Guilak, F., 1995, ''Compression-Induced Changes in the Shape and Volume of the Chondrocyte Nucleus,'' J. Biomech., **28**, pp. 1529–1541.
[3] Mow, V. C., Kuei, S. C., Lai, W. M., and Armstrong, C. G., 1980, ''Biphasic Creep and Stress Relaxation of Articular Cartilage in Compression? Theory and Experiments,'' J. Biomech. Eng., **102**, pp. 73–84.
[4] Spilker, R. L., de Almeida, E. S., and Donzelli, P. S., 1992, ''Finite Element Methods for the Biomechanics of Soft Hydrated Tissues: Nonlinear Analysis and Adaptive Control of Meshes,'' Crit. Rev. Biomed. Eng., **20**, pp. 279–313.
[5] Setton, L. A., Elliott, D. M., and Mow, V. C., 1999, ''Altered Mechanics of Cartilage with Osteoarthritis: Human Osteoarthritis and an Experimental Model of Joint Degeneration,'' Osteoarthritis Cartilage, **7**, pp. 2–14.
[6] Eckstien, F., Lemberger, B., Stammberger, T., Englmeier, K. H., and Reiser, M., 2000, ''Effect of Static Versus Dynamic in Vivo Loading Exercises on Human Patellar Cartilage,'' J. Biomech., **33**, pp. 819–825.
[7] Herberhold, C., Stammberger, T., Faber, S., Putz, R., Englmeier, K. H., Reiser, M., and Eckstein, F., 1998, ''An MR-Based Technique for Quantifying the Deformation of Articular Cartilage During Mechanical Loading in an Intact Cadaver Joint,'' Magn. Reson. Med., **39**, pp. 843–850.
[8] Gore, D. M., Higginson, G. R., and Minns, R. J., 1983, ''Compliance of Articular Cartilage and Its Variation through the Thickness,'' Phys. Med. Biol., **28**, pp. 233–247.
[9] Schinagl, R. M., Gurskis, D., Chen, A. C., and Sah, R. L., 1997, ''Depth-Dependent Confined Compression Modulus of Full-Thickness Bovine Articular Cartilage,'' J. Orthop. Res., **15**, pp. 499–506.
[10] Schinagl, R. M., Ting, M. K., Price, J. H., and Sah, R. L., 1996, ''Video Microscopy to Quantitate the Inhomogeneous Equilibrium Strain within Articular Cartilage During Confined Compression,'' Ann. Biomed. Eng., **24**, pp. 500–512.
[11] Eckstein, F., Tieschky, M., Faber, S., Englmeier, K. H., and Reiser, M., 1999, ''Functional Analysis of Articular Cartilage Deformation, Recovery, and Fluid Flow Following Dynamic Exercise in Vivo,'' Anat. Embryol. (Berlin), **200**, pp. 419–424.
[12] Eckstein, F., Tieschky, M., Faber, S. C., Haubner, M., Kolem, H., Englmeier, K. H., and Reiser, M., 1998, ''Effect of Physical Exercise on Cartilage Volume and Thickness in Vivo: MR Imaging Study,'' Radiology, **207**, pp. 243–248.
[13] Waterton, J. C., Solloway, S., Foster, J. E., Keen, M. C., Gandy, S., Middleton, B. J., Maciewicz, R. A., Watt, I., Dieppe, P. A., and Taylor, C. J., 2000, ''Diurnal Variation in the Femoral Articular Cartilage of the Knee in Young Adult Humans,'' Magn. Reson. Med., **43**, pp. 126–132.
[14] Hudelmaier, M., Glaser, C., Hohe, J., Englmeier, K. H., Reiser, M., Putz, R., and Eckstein, F., 2001, ''Age-Related Changes in the Morphology and Deformational Behavior of Knee Joint Cartilage,'' Arthritis Rheum., **44**, pp. 2556–2561.
[15] Regatte, R. R., Kaufman, J. H., Noyszewski, E. A., and Reddy, R., 1999, ''Sodium and Proton MR Properties of Cartilage During Compression,'' J. Magn. Reson Imaging, **10**, pp. 961–967.
[16] Herberhold, C., Faber, S., Stammberger, T., Steinlechner, M., Putz, R., Englmeier, K. H., Reiser, M., and Eckstein, F., 1999, ''In Situ Measurement of Articular Cartilage Deformation in Intact Femoropatellar Joints under Static Loading,'' J. Biomech., **32**, pp. 1287–1295.
[17] Rubenstein, J. D., Kim, J. K., and Henkelman, R. M., 1996, ''Effects of Compression and Recovery on Bovine Articular Cartilage: Appearance on MR Images,'' Radiology, **201**, pp. 843–850.
[18] Kaufman, J. H., Regatte, R. R., Bolinger, L., Kneeland, J. B., Reddy, R., and Leigh, J. S., 1999, ''A Novel Approach to Observing Articular Cartilage Deformation in Vitro via Magnetic Resonance Imaging,'' J. Magn. Reson Imaging, **9**, pp. 653–662.
[19] Mosher, T. J., and Smith, M. B., 1990, ''A DANTE Tagging Sequence for the Evaluation of Translational Sample Motion,'' Magn. Reson. Med., **15**, pp. 334–339.
[20] Axel, L., and Dougherty, L., 1989, ''Heart Wall Motion: Improved Method of Spatial Modulation of Magnetization for MR Imaging,'' Radiology, **172**, pp. 349–350.
[21] De Crespigny, A. J., Carpenter, T. A., and Hall, L. D., 1991, ''Cardiac Tagging in the Rat Using a DANTE Sequence,'' Magn. Reson. Med., **21**, pp. 151–156.
[22] McVeigh, E. R., 1996, ''MRI of Myocardial Function: Motion Tracking Techniques,'' Magn. Reson. Imaging, **14**, pp. 137–150.
[23] Duewell, S. H., Ceckler, T. L., Ong, K., Wen, H., Jaffer, F. A., Chesnick, S. A., and Balaban, R. S., 1995, ''Musculoskeletal MR Imaging at 4 T and at 1.5 T: Comparison of Relaxation Times and Image Contrast,'' Radiology, **196**, pp. 551–555.
[24] Mow, V. C., and Rosenwasser, M., 1988, ''Articular Cartilage: Biomechanics,'' in *Injury and Repair of the Musculoskeletal Soft Tissues*, S. L.-Y. Woo and J. A. Buckwalters, eds., American Academy of Orthopaedic Surgeons, Park Ridge, IL, pp. 427–463.
[25] Fung, Y. C., 1993, *Biomechanics: Mechanical Properties of Living Tissues*, Springer-Verlag, Inc., New York, NY.
[26] Haut, T. L., Hull, M. L., and Howell, S. M., 1998, ''A High-Accuracy Three-Dimensional Coordinate Digitizing System for Reconstructing the Geometry of Diarthrodial Joints,'' J. Biomech., **31**, pp. 571–577.
[27] Huang, A., Hull, M. L., Howell, S. M., and Haut Donahue, T. L., 2002, ''Identification of Cross-Sectional Parameters of Lateral Meniscal Allografts That

Predict Tibial Contact Pressure in Human Cadaveric Knees,'' ASME J. Biomech. Eng., **124**, pp. 481–489.
[28] Sekaran, S. V., Hull, M. L., and Howell, S. M., 2002, ''Nonanatomic Location of the Posterior Horn of a Medial Meniscal Autograft Implanted in a Cadaveric Knee Adversely Affects the Pressure Distribution on the Tibial Plateau,'' Am. J. Sports Med., **30**, pp. 74–82.
[29] Young, A. A., Axel, L., Dougherty, L., Bogen, D. K., and Parenteau, C. S., 1993, ''Validation of Tagging with MR Imaging to Estimate Material Deformation,'' Radiology, **188**, pp. 101–108.
[30] Martin, R. B., Burr, D. B., and Sharkey, N. A., 1998, *Skeletal Tissue Mechanics*, Springer-Verlag, Inc., New York, NY.
[31] Barker, M. K., and Seedhom, B. B., 1997, ''Articular Cartilage Deformation under Physiological Cyclic Loading—Apparatus and Measurement Technique,'' J. Biomech., **30**, pp. 377–381.
[32] Parkkinen, J. J., Lammi, M. J., Karjalainen, S., Laakkonen, J., Hyvarinen, E., Tiihonen, A., Helminen, H. J., and Tammi, M., 1989, ''A Mechanical Apparatus with Microprocessor Controlled Stress Profile for Cyclic Compression of Cultured Articular Cartilage Explants,'' J. Biomech., **22**, pp. 1285–1291.
[33] Steinmeyer, J., 1997, ''A Computer-Controlled Mechanical Culture System for Biological Testing of Articular Cartilage Explants,'' J. Biomech., **30**, pp. 841–845.
[34] Barker, M. K., and Seedhom, B. B., 2001, ''The Relationship of the Compressive Modulus of Articular Cartilage with Its Deformation Response to Cyclic Loading: Does Cartilage Optimize Its Modulus So as to Minimize the Strains Arising in It Due to the Prevalent Loading Regime?'', Rheumatology (Oxford), **40**, pp. 274–284.
[35] Armstrong, C. G., Lai, W. M., and Mow, V. C., 1984, ''An Analysis of the Unconfined Compression of Articular Cartilage,'' J. Biomech. Eng., **106**, pp. 165–173.